



Suspension Plasma Spray and Performance Characterization of Half Cells with NiO/YSZ Anode and YSZ Electrolyte

Y. Wang, J.-G. Legoux, R. Neagu, S. Hui, and B.R. Marple

(Submitted April 16, 2010; in revised form August 17, 2011)

The use of a liquid feedstock carrier in suspension plasma spray (SPS) permits injection of fine powders, providing the possibility of producing sprayed coatings that are both thin and dense and have fine microstructures. These characteristics make SPS an attractive process for depositing highly efficient electrodes and electrolytes for solid oxide fuel cell (SOFC) applications. In this study, NiO-yttria stabilized zirconia (YSZ) anode and YSZ electrolyte half cells were successfully deposited on porous Hastelloy X substrates by SPS. The NiO-YSZ anode deposition process was optimized by design of experiment. The YSZ electrolyte spray process was examined by changing one parameter at a time. The results from the design-of-experiment trials indicated that the porosity of the as-deposited coatings increased with an increase of suspension feed rate while it decreased with an increase of total plasma gas flow rate and standoff distance. The deposition rate increased with an increase of total plasma gas flow rate, suspension feed rate, and standoff distance. The microstructure examination by SEM showed that the NiO and YSZ phases were homogeneously distributed and that the YSZ phase had a lamellar structure. It was observed that the density of the YSZ electrolyte layer increased as input power of the plasma torch increased. Electrochemical characterization of the fabricated cells indicated that an open cell voltage of 0.989 V at 500 °C and a peak power of 0.610 W/cm² at 750 °C were reached.

Keywords NiO/YSZ anode, solid oxide fuel cells (SOFC), suspension plasma spray (SPS), YSZ electrolyte

1. Introduction

A solid oxide fuel cell (SOFC) is a highly efficient and clean energy conversion ceramic device that produces electricity by reaction of a fuel gas with an oxidant gas electrochemically. The basic physical structure of a fuel cell consists of a dense and gastight electrolyte layer in contact with a porous anode and cathode on either side. A composition consisting of 8 mol% yttria-stabilized zirconia (8YSZ) has been commonly used as electrolyte material due to its high ionic conductivity at high temperature while Ni/YSZ cermets are the most common anode materials used for SOFC applications. These cermets, in which YSZ provides ionic conduction and Ni provides electronic conduction, are attractive because of their relatively high catalytic activity, stability in hydrogen, and reasonable cost.

A wide range of SOFC manufacturing processes, such as tape casting and screen printing for planar designs, and

slip casting and extrusion for tubular designs, have been investigated by researchers around the world (Ref 1). Thermal plasma spray methods have been applied to the production of SOFC components for more than 40 years, e.g., to produce the electrode-electrolyte assembly of SOFCs by plasma spray (Ref 2). Among the different fabrication techniques, thermal spray shows a high potential for becoming an economic and high-quality production process for SOFCs, since it avoids the expensive and time-consuming sintering process that must be used by most other SOFC fabrication methods (Ref 3). However, it is difficult to produce the thin (<20 μm), fully dense layers required for SOFC electrolyte application by conventional powder plasma spraying, as plasma spray feedstock powder particles are typically between approximately 10 and 100 μm in diameter. In addition, the larger splats in conventional plasma sprayed coatings reduce the density of three-phase boundaries that are beneficial in the SOFC electrode application. As well, the lamellar microstructure of coatings formed by large splat stacking in conventional plasma spray will generate large residual defects and thermal stresses in SOFC components. All these features will negatively affect SOFC performance.

Suspension plasma spray (SPS), developed in recent years (Ref 4, 5), injects a suspension of the desired material into the plasma jet by an atomizing gas or high pressure. Because a liquid feedstock is employed as carrier, SPS permits the use of finer powders, on the nano- or submicron scale, than conventional thermal spraying. In SPS, heat and momentum transfer from the plasma to the suspension droplets leads to fragmentation and

Y. Wang, J.-G. Legoux, and B.R. Marple, Industrial Materials Institute, National Research Council of Canada, Boucherville, QC, Canada; and R. Neagu and S. Hui, Institute for Fuel Cell Innovation, National Research Council of Canada, Vancouver, BC, Canada. Contact e-mail: Youliangwang68@gmail.com.

acceleration of the suspension droplets, the evaporation and/or combustion of the solvent, and condensation and/or melting of the suspension materials, resulting in the formation of a coherent deposit. The splats produced by SPS are much smaller than those of conventional plasma spray (Ref 6, 7), providing the possibility of producing sprayed coatings that are both thin and dense and have fine microstructures. The smaller splats in suspension plasma sprayed porous coatings will increase the occurrence of three-phase boundaries in the electrode, a result that can be advantageous for performance in SOFC applications. The dense coatings produced by SPS have a much more homogeneous microstructure, and no splat stacking can be observed (Ref 8, 9), which is desirable for the electrolyte in SOFC applications. In brief, the SPS process has the potential to deposit highly efficient electrodes and electrolytes for SOFCs.

In our previous study, SOFCs based on a Sm-doped ceria (SDC) electrolyte and NiO-SDC anode have been successfully fabricated by SPS (Ref 10, 11). In this study, deposition of porous Ni-YSZ anodes and dense YSZ electrolytes on porous Hastelloy has been demonstrated by SPS using an axial injection plasma torch. The porous Ni-YSZ anode deposition process was optimized by a design-of-experiment technique. The parameters for dense YSZ electrolyte deposition were selected by changing one parameter at a time to identify the optimum deposition conditions. After selection of optimized conditions, anode and electrolyte half cells were produced and the deposited coatings characterized by scanning electron microscope (SEM). After applying $\text{Ba}_{0.5}\text{Pr}_{0.5}\text{Co}_{0.8}\text{Fe}_{0.2}\text{O}_{3-\delta}$ (BPCF) cathode paste by stencil printing on the surface of YSZ electrolyte, the fabricated SOFCs were characterized electrochemically.

2. Experimental Procedure

2.1 Suspension Spray Setup

SPS was carried out using an axial injection plasma torch (Mettech Axial III, Northwest Mettech Corp., North Vancouver, BC, Canada). An internal injection and twin-fluid atomization module was installed in the plasma torch for atomization of suspension liquid into droplets and injecting them into the plasma jet axially. With this design, the suspension droplets are fully entrained in the three encircling plasma jets of the Mettech Axial III torch. Such a configuration can increase the transfer of heat and momentum from the plasma jets to the injected droplets. The suspension was transported into the plasma jet by a prototype feeder (Nanofeed Liquid Powder Feeder, Model 640, Northwest Mettech, North Vancouver, Canada), which enables automatic computer control of the suspension flow rate, start-up, shut-down, and rinsing. Nitrogen, at a flow rate of 10 slpm, was used as the atomizing gas.

The temperature and velocity of in-flight particles in these SPS trials were measured with a commercial diagnostic system (AccuraSpray[®] G2, Tecnar, St-Bruno, QC,

Canada). During the measurement, the sensor of the AccuraSpray[®] G2 was focused on the center of the plasma jet at the location where the substrate would be positioned during deposition.

The substrates were held on an electrically heated substrate holder which was capable of heating the substrate to temperature between 23 and 700 °C. Air-forced jets were used to cool the front surface of the substrate. The substrate temperature was measured using an optical pyrometer.

2.2 Suspensions and Substrates

A suspension containing 9 wt.% of a solids mixture composed of NiO (fuelcellmaterials.com, Lewis Center, OH, USA) and YSZ (Inframat[®] Advanced Materials, Farmington, CT, USA) in 30 wt.% ethylene glycol (A&C American Chemicals Ltd. Montreal, Canada) and 70 wt.% ethanol was used in anode deposition. The weight percentages of NiO and YSZ in the solid mixture were 55 and 45, respectively. After reducing NiO to Ni, the anode was expected to contain 40 vol.% Ni and 60 vol.% YSZ. In order to produce high porosity in the fabricated coating, a NiO powder having a relatively large particle size, with a d_{50} of 14.4 μm and a specific surface area of 0.21 m^2/g , was employed. The YSZ powder had a d_{50} of 0.5 μm and specific surface area of 40 m^2/g . In the electrolyte deposition, suspensions containing 3, 5, and 7 wt.% YSZ nanopowder (Inframat[®] Advanced Materials, Farmington, CT, USA) in 70 wt.% ethylene glycol and 30 wt.% ethanol were employed. The YSZ nanopowder had a d_{50} of 30-60 nm and a specific surface area of 15-40 m^2/g . All the suspensions were prepared with the addition of polyethyleneimine (MWT 25,000 Alfa Aesar, USA) as dispersing agent.

Tape cast and sintered Hastelloy X plates with a porosity of 25.7% (Mott Corp., Farmington, CT, USA) were used as substrates and served as the supporting layer for the SOFCs. Hastelloy X is a Ni-Cr-Fe-Mo alloy with high oxidation resistance.

2.3 Spray Parameters for NiO-YSZ Deposition

The microstructure requirement for anode operation is 30-40% porosity to facilitate fuel gas and reaction product transport, and provide the reaction sites (three-phase boundaries) required for electrode chemical reaction (Ref 12). To produce porous anodes, a relatively low plasma torch power (61-67 kW) with a secondary plasma gas containing 30% helium was used to generate lower plasma temperature and less efficient heating of injected feedstock. In addition, NiO powder was employed, instead of Ni, in the Ni-YSZ anode deposition process. It was expected that, after reduction of the NiO to Ni, 23% additional porosity could be created in the anode layer.

To identify conditions for producing coatings with a porosity level suitable for the SOFC anode application at high deposition rate, a factorial design of experiment was used to optimize the anode deposition process (Ref 13). Based on preliminary trials, total plasma gas flow rate,

suspension flow rate and standoff distance were selected as the critical factors because of their importance in deciding the responses, i.e., deposition rate and coating porosity (Ref 14-16). The deposition rate (thickness/pass) was defined as the increase in coating thickness per pass of the spray jet, and the porosity, represents the as-deposited NiO-YSZ coating's porosity measured at a magnification of 600× by SEM. As shown in Table 1, two levels were used for each factor and eight coatings were deposited for the experiment design. For a given gas composition and power setting, the total plasma gas flow rate determines the velocity and temperature of the plasma jet (Ref 16); therefore, it will affect the microstructure of fabricated coatings. For a given system, the size and density of generated particles in the plasma jet are determined by the suspension flow rate, which greatly influences the deposition process (Ref 14-16). Since the small particles generated in SPS carry little momentum and low thermal inertia, relatively short standoff distances (5.08 and 6.35 cm) were identified as being appropriate in preliminary trials.

Eleven spray conditions, as listed in columns 2-5 in Table 2, were used to optimize the YSZ electrolyte deposition process by changing values for plasma torch power input, suspension flow rate, suspension concentration, and standoff distance one at a time. These parameters were selected based on preliminary trials.

The as-deposited NiO-YSZ anode coatings were reduced in hydrogen before deposition of YSZ electrolyte

Table 1 Experiment design matrix for NiO-YSZ anode deposition

No	Total gas, L/min	Feed rate, kg/h	Standoff distance, cm	Thickness / pass, μm	Porosity, %
1	225	2	5.1	0.40	3.3
2	275	2	5.1	0.69	1.1
3	225	3	5.1	0.56	5.5
4	275	3	5.1	0.86	2.8
5	225	2	6.4	0.74	1.7
6	275	2	6.4	0.71	1.0
7	225	3	6.4	0.90	3.5
8	275	3	6.4	0.99	2.4

Table 2 Spray parameters for YSZ electrolyte deposition and the porosity level of the coatings

No	Power, kW	Standoff distance, cm	Feed rate, kg/h	Suspension concentration, wt. %	T, °C	V, m/s	Porosity, %
1	93	5.1	2	3	3105	638	2.5
2	93	5.1	2	5	3074	637	0.8
3	93	6.4	2	5	3058	596	2.3
4	95	5.1	2	3	3055	777	0.4
5	95	5.1	2	5	2993	778	0.6
6	95	6.4	2	5	2977	719	0.4
7	108	5.1	2	3	3092	794	0.4
8	108	5.1	2	5	3047	787	0.1
9	108	6.4	2	5	3033	737	0.3
10	108	6.4	2.5	5	2971	720	0.4
11	108	6.4	2	7	3031	741	0.2

coatings, by increasing the temperature at 5 °C/min from room temperature to 650 °C, holding at 650 °C for 1 h, and then decreasing the temperature at 5 °C/min from 650 °C to room temperature.

2.4 Coating Characterization

The coating microstructures were examined by SEM (JSM-610, JEOL Tokyo, Japan) and field-emission SEM (FE-SEM) (S4700, Hitachi, Tokyo, Japan). The samples were prepared by standard metallographic methods to produce a polished cross section. To determine the phases present, x-ray diffraction (XRD) analyses (Bruker D8 Advance Diffractometer equipped with a Vântec Detector, Karlsruhe, Germany) were performed on as-deposited coatings using Cu K α radiation. Porosity was measured on the polished cross section by SEM (600× for anode and 5000× for electrolyte) using image analysis. Fifteen measurements for anode coatings and ten measurements for electrolyte coatings were averaged per sample.

2.5 Cathode Deposition and Fuel Cell Test

The half cells were tested for helium leak rate at 1 psi differential pressure. Ba_{0.5}Pr_{0.5}Co_{0.8}Fe_{0.2}O_{3- δ} (BPCF) cathode paste was stencil printed on the half cell using a 13 mm diameter mask as shown in Fig. 1 and sintered in situ at 800 °C for 2 h, in air, while the anode was maintained under nitrogen. To reduce NiO to Ni in the anode, the cell temperature was subsequently brought to and maintained at 650 °C for 5 h while gradually increasing hydrogen concentration in the anodic compartment, i.e., 10% H₂ for 90 min, 20% H₂ for 60 min, 50% H₂ for 30 min, and 100% H₂ for 120 min. The polarization curves were measured between 500 and 750 °C at 50 °C intervals. Electrochemical impedance spectroscopy (EIS) was used to measure ohmic and polarization resistances. For each temperature in the above-mentioned range, an EIS

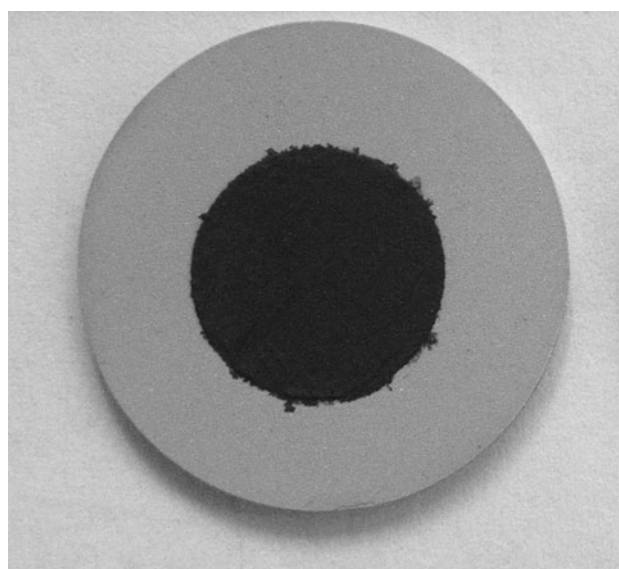


Fig. 1 Optical photographs of the fabricated fuel cell

spectrum have been acquired at OCV, over the 0.1 to 100 kHz frequency range, with a 50 mV AC excitation. A Solartron 1480 multistat coupled with a Solartron 1260 frequency response analyzer (Solartron Analytical, Oak Ridge, USA) was used to characterize the half cells, using humidified hydrogen (3 vol.% H₂O) as fuel and air as the oxidant.

3. Results and Discussion

3.1 Anode Deposition

As shown in Table 1, values for the deposition rate are between 0.40 and 0.99 $\mu\text{m}/\text{pass}$ and the as-deposited NiO-YSZ coatings have porosity levels between 1.0 and 5.5%. After reducing the NiO to Ni, the anode layer porosity level is expected to be 24-28.5%. During anode deposition, the substrate temperatures were 200-300 °C by using water-cooled substrate holder and air jets cooling. The power of plasma torch is 68 kW.

Figure 2(a) shows back-scattered SEM images of the microstructures of the as-deposited NiO-YSZ coatings. It can be seen in Fig. 2(a) that there are two phases, as

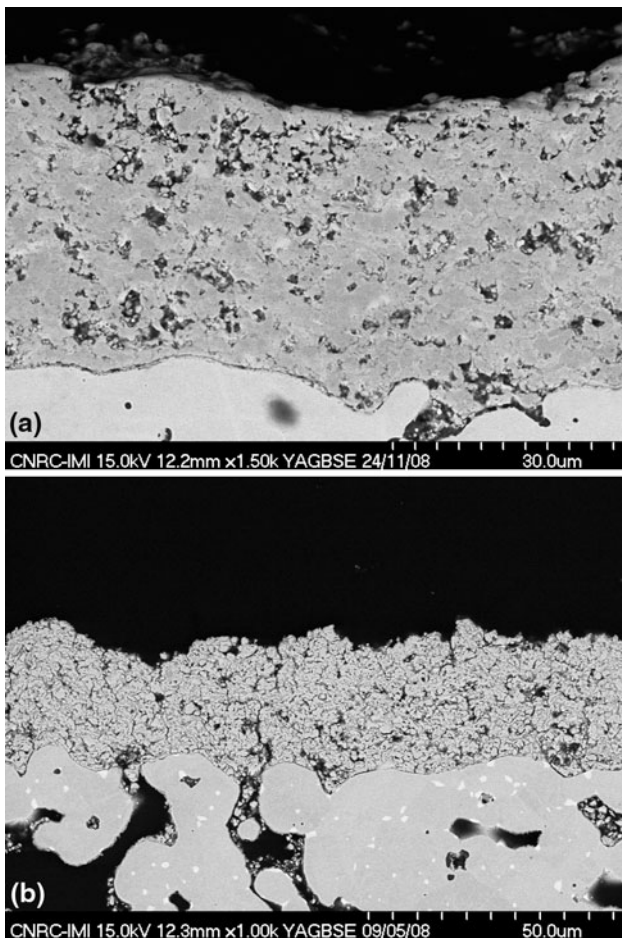


Fig. 2 SEM images of the NiO-YSZ (a) and the reduced Ni-YSZ anodes (b) deposited at optimized conditions

represented by the light- and dark-gray regions, in the as-deposited coating. EDX analysis indicates that the white phase is YSZ and the dark phase is NiO. Figure 2(a) shows that the distribution of the YSZ and NiO phases are relatively homogeneous and that the YSZ phase has a lamellar structure. Figure 2(b) is SEM image of the Ni-YSZ anode reduced in hydrogen before deposition of YSZ electrolyte coatings, by increasing the temperature at 5 °C/min from room temperature to 650 °C, holding at 650 °C for 1 h, and then decreasing the temperature at 5 °C/min from 650 °C to room temperature. Figure 2(b) indicates that the reduced coatings are porous and the pore distribution is homogeneous. The XRD spectrum of the anode layer (lower spectrum of Fig. 3) shows the presence of well-crystallized cubic zirconia, cubic NiO, and metallic nickel. The presence of metallic nickel is the result of the partial reduction of NiO in the hydrogen-rich plasma environment or may originate from the Ni signal in the Hastelloy X substrate, given the $\sim 30 \mu\text{m}$ thickness of the anode layer.

3.1.1 Results of Experiment Design for NiO-YSZ Anode Deposition. The results of deposition rate and porosity measurements were analyzed by commercial experiment design software (Design Expert 7.1.6) (Ref 17). The software can calculate the half-normal plot and analysis of variance (ANOVA) of the responses (Ref 13). Figure 4 shows the half-normal plot of the response, deposition rate (thickness/pass). If the estimates of the main factor effects and the effects of interactions have no influence on the responses, the points will fall approximately on a straight line passing through the origin in the figure. By contrast, points that fall well off the line to the right at the top would indicate the existence of real effects (Ref 13). Therefore, the half-normal plot in Fig. 4 suggests that changes in main factors A (total gas flow), B (suspension feed rate), and C (standoff distance), and the interaction between factors A (total gas flow) and C (standoff distance) have significant effects on the measured response (thickness/pass). According to the

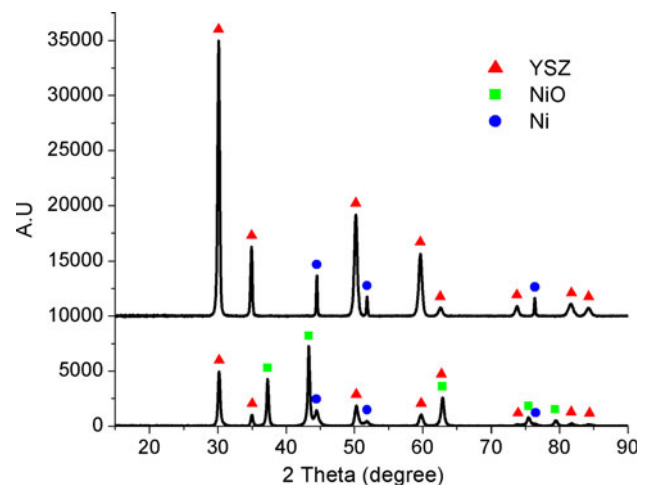


Fig. 3 XRD of as-deposited coatings (anode: lower spectrum, electrolyte: upper spectrum)

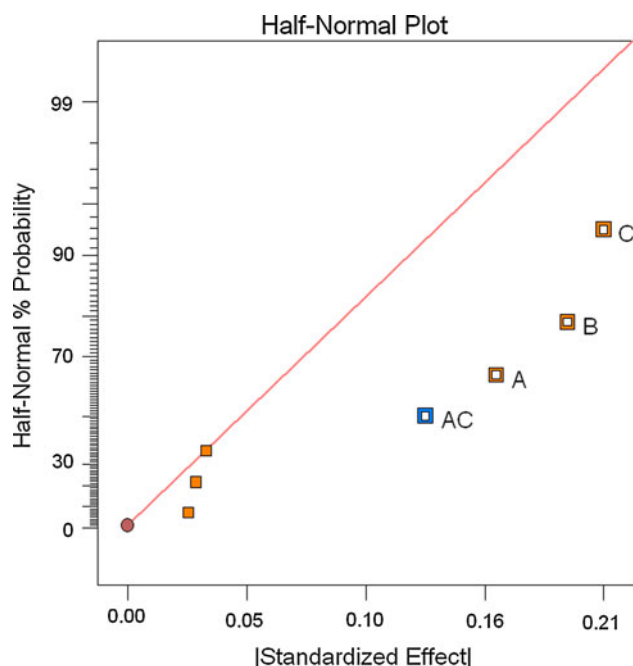


Fig. 4 Half-normal plots for deposition rate

ANOVA analysis by the software, the deposition rate can be expressed by the following equation:

$$\text{Thickness/pass} = 0.73 + 0.081A + 0.096B + 0.10C - 0.065AC \quad (\text{Eq 1})$$

The equation indicates that the thickness/pass increases with the increase of total plasma gas flow rate, suspension feed rate, and standoff distance and it decreases as the interaction between total gas flow rate and standoff distance increases. The half-normal plot of porosity (not presented) showed that the total gas flow rate, suspension feed rate, and standoff distance had a significant effect on coating porosity. The porosity level in the as-deposited coatings can be written as

$$\text{Porosity} = 2.66 - 0.84A + 0.89B - 0.51C + 0.39AC \quad (\text{Eq 2})$$

Equation 2 shows that the porosity of the as-deposited coatings is linearly proportional to the suspension feed rate (B) and to the interaction between total plasma gas flow (A) and standoff distance (C) while it decreases with the increase of total plasma gas flow (A) and standoff distance (C).

Within the experimental area in which NiO-YSZ deposits can be produced, the deposition process was optimized by the experiment design software based on the analyses described in previous sections. The criteria for the optimization process were based on the microstructure requirements for the SOFC anode and the production cost. The microstructural requirement for the anode was to maximize the level of porosity in this project. To identify the most condition that provided the maximum production rate, the process that yielded the highest

Table 3 Optimized parameter for NiO and YSZ anode deposition

Total gas, L/min	Feed rate, kg/h	Standoff distance, cm
225	4.0	6.2

deposition rate (thickness/pass) needed to be identified. The optimization analysis on the above conditions generated 38 processing parameter combinations for maximizing these two responses (porosity and thickness/pass). A parameter combination of total plasma gas = 225 L/min, suspension feed rate = 4 kg/h, and standoff distance = 6.2 cm (as shown in Table 3) was used to deposit anode coatings since this parameter combination is the best one in optimizing the two responses as determined by the desirability function (Ref 13). Figure 2 shows the SEM micrographs of NiO-YSZ and reduced Ni-YSZ anode coating deposited at this optimized condition.

3.2 Electrolyte Deposition

YSZ electrolyte coatings were deposited at 11 spray conditions by changing one parameter at a time as shown in Table 2. Figure 5 shows the SEM images of coatings deposited using Nos. 1, 4, and 7 spray conditions in Table 2. As shown in Table 2, the plasma torch input power for spray condition Nos. 1-3, Nos. 4-6, and Nos. 7-11 are 93, 95, and 108 kW, respectively, and the total gas flow rate, plasma composition, and current are the same in spray condition Nos. 1-3, Nos. 4-6, and Nos. 7-11, respectively. By comparing Nos. 1, 4, and 7 of Fig. 5, it is found that the coatings become denser with an increase of plasma torch input power. The porosity measurements show that coating Nos. 1-3, Nos. 4-6, and Nos. 7-11 have an average porosity of 1.8, 0.5, and 0.3%, respectively, which is consistent with the result of the picture comparison. For example, this can be seen by comparing the results shown in rows 1, 4, and 7 in Table 2 and the corresponding photos in Fig. 5 (Nos. 1, 4, and 7). The temperature and velocity measurements from particle diagnostics show that there is no significant change in average particle temperature as the plasma torch input power is increased; however, the particle velocity is greater at higher plasma torch input power, as shown in Table 2. The higher particle velocity improves the impaction of the molten particles and increases the density of coatings.

By comparisons of the porosities of coatings deposited at condition Nos. 1 and 2, Nos. 4 and 5, and Nos. 7 and 8, respectively, as shown in Table 2, it is found that suspension concentration has no significant effect on the fabricated coating's density. In the same way, by comparing the porosity data in Table 2, it is demonstrated that changing the standoff distance from 5.1 to 6.3 cm has no significant effect on the porosity of coatings, although the particle velocity at a standoff distance of 6.3 cm is smaller than that of 5.1 cm. The corresponding porosities of coating Nos. 9 and 10 in Table 2 are approximately the

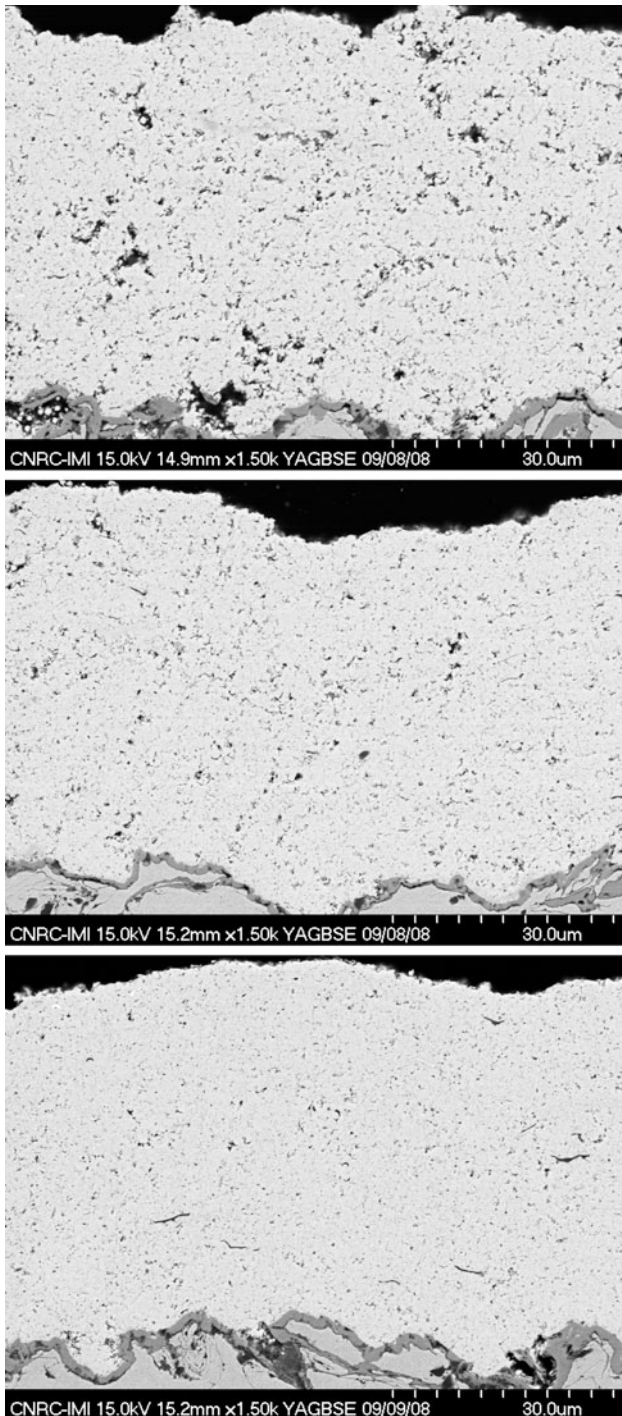


Fig. 5 SEM images of electrolyte coatings deposited at selected conditions of Nos. 1, 4, and 7 (from top to bottom, respectively. Pictures of other conditions are not presented.) in Table 2

same, indicating that suspension feed rate has no significant effect on porosity. In brief, suspension concentration and suspension flow rate show no significant effect on coating porosity at the standoff distances used in our experiments; however, higher plasma torch input power produces YSZ coatings with lower porosity in the investigated ranges of spray parameters.

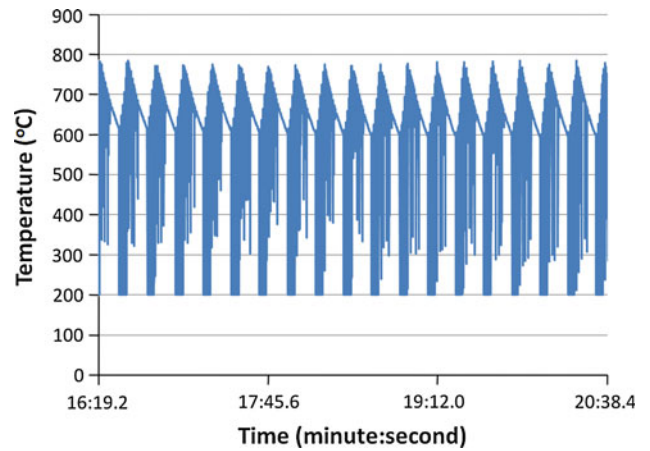


Fig. 6 Substrate temperature during electrolyte deposition

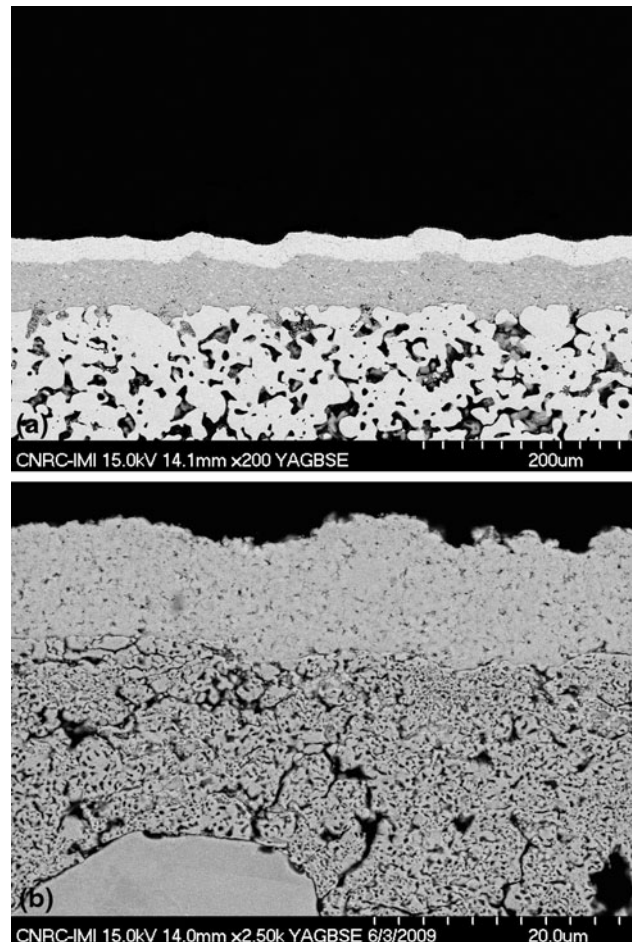


Fig. 7 SEM pictures of cross sectioned half cells

3.3 Half Cell Deposition

Ni-YSZ anode and YSZ electrolyte half cells were deposited at the conditions optimized in the previous sections. The as-deposited NiO-YSZ coatings produced using the conditions in Table 3 were lightly polished to

remove the humps on the surface to facilitate electrolyte deposition. The polished NiO-YSZ coatings were heat-treated in hydrogen to reduce the NiO to Ni. The YSZ electrolyte coatings were deposited using spray parameter set No. 9 in Table 2. This condition had a combination of a larger standoff distance and a smaller suspension flow rate, which could reduce variation of the substrate temperature so vertical cracks observed in some deposited coatings produced at other conditions could be removed. Figure 6 shows the substrate temperature during electrolyte coating deposition at the optimized condition, which indicates that the maximum substrate temperature was about 800 °C. The 5% suspension concentration used in condition 9 was found to be appropriate for the suspension feeding system. The fabricated YSZ electrolyte coatings were about 10-20 μm in thickness. No vertical cracks were observed in deposited electrolytes. Figure 7 shows a SEM image of a deposited half cell on a porous Hastelloy X substrate, indicating that the anode is porous and the electrolyte is dense. Interconnected pores were not observed in the electrolyte layer. XRD analysis of the as-deposited electrolyte (upper spectrum of Fig. 3) shows cubic YSZ and metallic Ni are present. The Ni peaks result from the Ni in the reduced anode since the YSZ coating used for XRD is only ~ 10 μm thick.

3.4 Cell Evaluation

The leak rates of half cells deposited at the optimized conditions were measured using He gas with a differential pressure of 1 psi. The measurement result shows that the specific leak rate for a half cell with a 40 μm thick anode

and a 20 μm thick YSZ electrolyte reached 0.058 SCCM/cm².

After BPCF cathode paste was stencil printed on the half cell and fired in situ at 800 °C for 2 h to form the SOFC, power generation characteristics and AC impedance measurements of the fabricated cells were performed between 500 and 750 °C with an interval of 50 °C using humidified hydrogen as fuel and air as oxidant. Figure 8 shows power density and cell voltage as a function of current density. The highest open circuit voltage (OCV) is 0.989 V at 500 °C, which is higher than those obtained for cells with HVOF-suspension-deposited 30 μm SDC electrolyte (Ref 10) or a suspension-plasma-deposited 30 μm SDC electrolyte (Ref 18) produced previously. The higher OCV indicates that 20 μm YSZ electrolyte layers produced in this project are more gas tight than a HVOF-suspension-deposited 30 μm SDC electrolyte (Ref 10) and a suspension-plasma-deposited 30 μm SDC electrolyte (Ref 18). The OCV value of 0.989 V is lower than the theoretical OCV value because the 20 μm YSZ electrolyte is not fully gas tight. As the temperature increases, the OCV decreases linearly, as shown in Fig. 9.

The maximum power density reached 0.610 W/cm² at 750 °C. This performance compares very favorably with the previous results from the same laboratory (Ref 18), as well as other published results for SOFCs with YSZ as electrolyte. Meng et al. (Ref 19) fabricated YSZ electrolyte coatings implementing electron-beam physical vapor deposition combined with a sol infiltration treatment and reached maximum output powder density of 150 mW cm⁻² at 800 °C. Young et al. (Ref 20) reached power densities of 175 mW cm⁻² at 750 °C for cells with

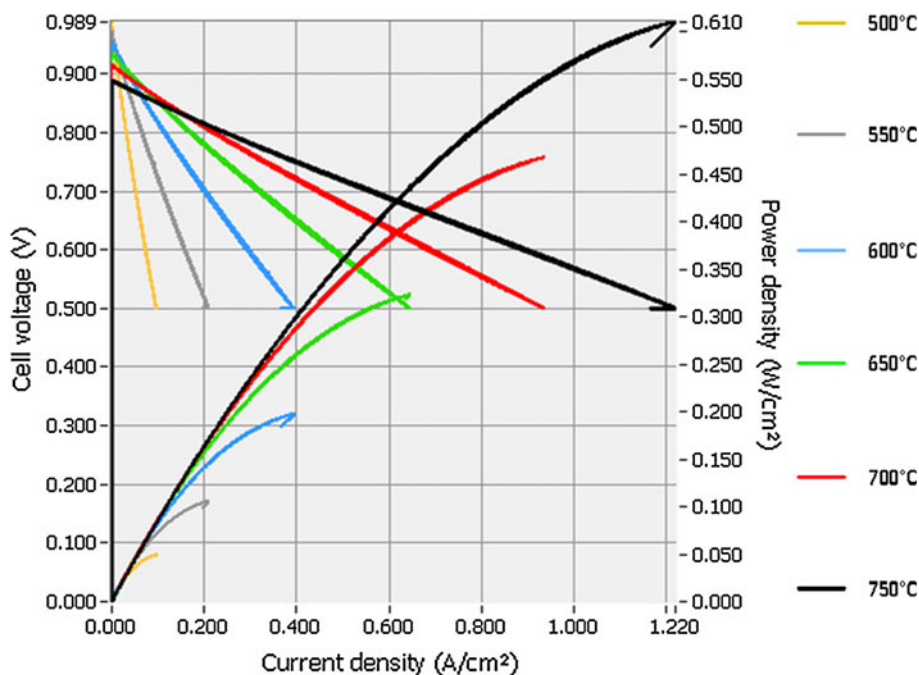


Fig. 8 Power density and cell voltage as function of current density between 500 and 750 °C for a cell of 40 μm Ni-YSZ anode/20 μm YSZ electrolyte/stencil printed BPCF No. 3 cathode

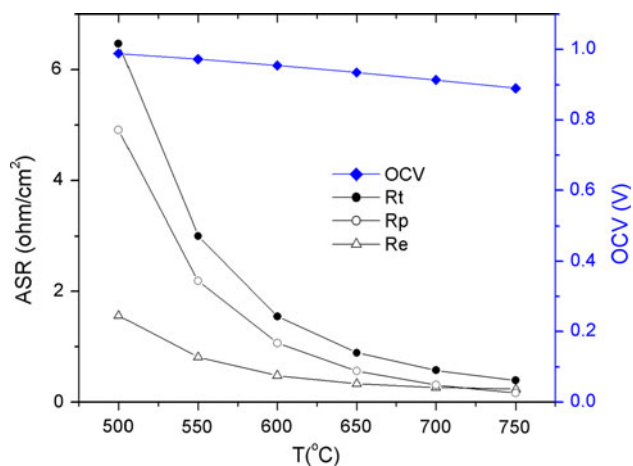


Fig. 9 Area-specific resistances (ASR) (R_t , total resistance; R_p , polarization resistance; R_e , ohmic resistance) and open circuit voltage (OCV) of a fabricated cell as a function of temperature T

inkjet-printed YSZ electrolyte layers. Bao et al. (Ref 21) used an electrostatic powder-coating process to fabricate dense YSZ electrolyte coatings on a Ni-YSZ support and reached power densities of 142 mW cm^{-2} at $750 \text{ }^\circ\text{C}$.

Figure 9 shows the area specific resistances (ASRs) as a function of temperature T ($^\circ\text{C}$). Above $650 \text{ }^\circ\text{C}$, both the polarization resistance (R_p) and ohmic resistance (R_e) were relatively small, which means that the catalytic activity of the electrodes is sufficient and the ohmic resistance of the cell components is smaller at higher temperature. At lower temperatures, however, both ohmic and polarization resistance increase significantly. Higher ohmic resistance is generally due to lower ionic conductivity of the electrolyte layer at lower temperatures or may be a consequence of poor electrode/electrolyte contact in cells. The high polarization resistance, R_p , may result from imperfect contact between the electrolyte and the electrodes or a reduced area of three-phase (Ni/YSZ/ O_2 gas) boundaries.

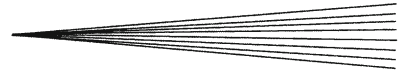
4. Conclusion

Ni-YSZ anode and YSZ electrolyte half cells were successfully deposited on porous Hastelloy X substrates by SPS. The thickness of the anode and electrolyte layers was $\sim 40 \text{ }\mu\text{m}$ and $10\text{-}20 \text{ }\mu\text{m}$, respectively. The NiO-YSZ coating deposition process was optimized by design of experiment. The YSZ electrolyte spray process was examined by changing one parameter at a time. The results from the design of experiment indicate that the porosity level in the deposited anode coatings increased with the increase of suspension feed rate while it decreased with the increase of total plasma gas flow and standoff distance. The deposition rate increased with an increase of total gas flow rate, suspension feed rate, and standoff distance. The density of YSZ electrolyte coatings increased as plasma torch input power increased. The anodes of the deposited half cells were porous. The

electrolytes were dense, with no interconnected pores. XRD analyses of the as-deposited layers detected cubic YSZ, NiO, and Ni in the anode and cubic YSZ in the electrolyte. Evaluation of the electrochemical performance of these layers indicated that an open cell voltage of 0.989 V at $500 \text{ }^\circ\text{C}$ and a peak power of 0.610 W/cm^2 at $750 \text{ }^\circ\text{C}$ were reached.

References

1. F. Tietz, H.-P. Buchkremer, and D. Stover, Components Manufacturing for Solid Oxide Fuel Cells, *Solid State Ion.*, 2002, **152-153**, p 373-381
2. H. Tannenberger and R. Schmitt, Swiss Patent No. 491 510,31
3. R. Henne, M. Lang, M. Muller, R. Ruckdaschel, and G. Schiller, Manufacturing of Solid Oxide Fuel Cells—A Challenge for DC and RF Plasma Deposition Processes, *Heat and Mass Transfer Under Plasma Conditions*, Vol 891, P. Fauchais, J.V.D. Mullen, and J. Heberlein, Ed., The New York Academy of Sciences, New York, 1999, p 124-136
4. P. Fauchais, R. Etchart-Salas, V. Rat, J.F. Coudert, N. Caron, and K. Wittmann-Teneze, Parameters Controlling Liquid Plasma Spraying: Solutions, Sols, or Suspensions, *J. Therm. Spray Technol.*, 2008, **17**(1), p 31-59
5. F. Gitzhofer, E. Bouyer, M.I. Boulos, US Patent 5609921, 1997
6. P. Blazdell and S. Kuroda, Plasma Spraying of Submicron Ceramic Suspensions Using a Continuous Ink Jet Printer, *Surf. Coat. Technol.*, 2000, **123**, p 239-246
7. J. Fazilleau, C. Delbos, M. Violier, J-F. Coudert, and P. Fauchais, Influence of Substrate Temperature on Formation of Micrometric Splats Obtained by Plasma Spraying Liquid Suspension, *Thermal Spray 2003: Advancing the Science & Applying the Technology*, B.R. Marple and C. Moreau, Ed., 5-8 May 2003 (Materials Park, Ohio, USA), ASM International, p 889-893
8. P. Fauchais, R. Etchart-Salas, C. Delbos, M. Tognonvi, V. Rat, J.F. Coudert, and T. Chartier, Suspension and Solution Plasma Spraying of Finely Structured Layers: Potential Application to SOFCs, *J. Phys. D*, 2007, **40**, p 2394-2406
9. C. Delbos, J. Fazilleau, J.F. Coudert, P. Fauchais, and L. Bianchi, Plasma Spray Elaboration of Finely Structured YSZ Thin Coating by Liquid Suspension Injection, *Thermal Spray 2003: Advancing the Science & Applying the Technology*, B.R. Marple and C. Moreau, Ed., ASM International, Materials Park, Ohio, USA, 2003, p 661-669
10. J.O. Berghaus, J.-G. Legoux, C. Moreau, R. Hui, C. Decès-Petit, W. Qu, S. Yick, Z. Wang, R. Maric, and D. Ghosh, Suspension HVOF Spraying of Reduced Temperature Solid Oxide Fuel Cell Electrolyte, *J. Therm. Spray Technol.*, 2008, **17**(5-6), p 700-707
11. R. Hui, J.O. Berghaus, C. Decès-Petit, W. Qu, S. Yick, J.G. Legoux, and C. Moreau, High Performance Metal-Supported SOFCs Fabricated by Thermal Spray, *J. Power Sour.*, 2009, **191**, p 371-376
12. W.Z. Zhu and S.C. Deevi, A Review on the Status of Anode Materials for Solid Oxide Fuel Cells, *Mater. Sci. Eng.*, 2003, **A362**, p 228-239
13. R.H. Myers and D.C. Montgomery, *Response Surface Methodology, Process and Product Optimization Using Designed Experiments*, 2nd ed., John Wiley & Sons, Inc., New York, 2002
14. Y. Wang and T.W. Coyle, Solution Precursor Plasma Spray of Nickel-Yttria Stabilized Zirconia Anodes for Solid Oxide Fuel Cell Application, *J. Therm. Spray Technol.*, 2007, **16**(5-6), p 899-904
15. Y. Wang and T.W. Coyle, Optimization of Solution Precursor Plasma Spray Process by Statistical Design of Experiment, *J. Therm. Spray Technol.*, 2008, **17**(5-6), p 692-699
16. Y. Wang, Deposition of Solid Oxide Fuel Cell Electrodes by Solution Precursor Plasma Spray, Ph. D. Thesis, University of Toronto, 2008
17. <http://www.qualitycoach.net/land/designexpert.html>, 2009
18. Z. Wang, J.O. Berghaus, S. Yick, C. Decès-Petit, W. Qu, R. Hui, R. Maric, and D. Ghosh, Dynamic Evaluation of



- Low-Temperature Metal-Supported Solid Oxide Fuel Cell Oriented to Auxiliary Power Units, *J. Power Sour.*, 2008, **176**, p 90-95
19. B. Meng, X. He, Y. Sun, and M. Li, Preparation of YSZ Electrolyte Coatings for SOFC by Electron Beam Physical Vapor Deposition Combined With a Sol Infiltration Treatment, *Mater. Sci. Eng.*, 2008, **B 150**, p 83-88
 20. D. Young, A.M. Suresh, R. Cummins, H. Xiao, M. Rottmayer, and T. Reitz, Ink-Jet Printing of Electrolyte and Anode Functional Layer for Solid Oxide Fuel Cells, *J. Power Sour.*, 2008, **184**, p 191-196
 21. W. Bao, W. Zhu, G. Zhu, J. Gao, and G. Meng, Dense YSZ Electrolyte Films Prepared by Modified Electrostatic Powder Coating, *Solid State Ion.*, 2005, **176**, p 669-674